KAPITEL 3 / *CHAPTER 3* [3]
DESIGN AND MODELLING OF A CHAOTIC TRANSCEIVER FOR FREQUENCY OUTPUT QUARTZ TRANSDUCERS

DOI: 10.30890/2709-2313.2024-29-00-032

Introduction

The application of unidirectional synchronization of two coupled Chen systems is exhibited in this chapter. In spite of the high dependence on initial conditions, which means that two initially close phase trajectories with time become uncorrelated, it is possible to synchronize two dynamical systems in order to make them evolve identically. Data transmitting using chaos requires mixing an information signal with a chaotic carrier. This procedure performs data encryption and spreads the spectrum of an information signal, which increases information security and reliability. Thus, the prospect of using devices with chaotic dynamics in modern telecommunication and telemetry applications is due to several factors, including high information capacity, a wide range of frequencies, and confidentiality of messages. The proposed scheme is considered to be used in a measuring transducer design which requires sensors to operate at a long distance from the rest of the scheme. We propose an application of a chaotic oscillator as a transceiver module for a quarts sensor transducer, which could be used in a telemetry application. The process of producing non-periodic but determined oscillations by the non-linear Chen system and signal transmission application, based on it, are the subject of the research. The complete synchronization of two unidirectionally connected Chen systems and its signal transmitting application are considered. The goal is to develop a transceiver extension for the quartz measuring transducer scheme to ensure the stable operating of sensors at a long distance from the rest of the scheme. The result of the research: the chaos synchronization scheme has been applied to transmit a frequency modulated signal, obtained from a difference-frequency block of pressure quartz sensor transducer. Additionally, the mathematical model and numerical modeling of the Chen dynamical system have been done. The numerical solution of the system's differential equations was calculated using Matlab software. In order to study the change in the dynamic regime

[3]**Authors:** *Pidchenko Serhii, Taranchuk Alla, Slobodian Maksym*

depending on the parameters of the model, the spectrum of Lyapunov exponents was calculated and bifurcation diagrams were constructed. The circuit design of the Chen oscillator was built using Multisim software, which uses the PSpice model to simulate electrical components. A model of an analog signal transmission system with chaotic mixing of a frequency output signal with a chaotic carrier has been proposed as an extension of the use of quartz transducers in measuring devices.

3.1. Literature overview of the topic

The process of designing and modeling of measuring transducers design assigns many technological and constructing tasks, e.g., ensuring high transformation performance, high measurement accuracy, strong noise tolerance, linear transfer characteristics, high level of an output signal, etc [1-4]. Technical invariance of quartz crystal oscillators to destabilizing factors (DF) of the environment can be ensured by using the resonator in a multi-frequency mode [5, 6]. Thus, e.g., the quartz pressure transducer, which has been described in the work [7], can operate in either single- or the multi-frequency mode of the quartz resonator.

Additionally, in telemetry systems design, quartz sensors are often required to operate at a long distance from the rest of the transducer scheme, which leads to increased noise immunity requirements [1-4], which is a crucial factor to ensure stability and prevent failure of end-user devices [8]. To manage this issue, in this paper, we propose an application of a chaotic oscillator as a transceiver module for quarts sensor transducer, which could be used in telemetry systems designs.

Having been discovered in 60th, the phenomenon of producing non-periodic noise-like complex signals by completely deterministic systems is thought to be one of the most significant scientific breakthroughs of the 20th century. First noticed by Lorenz in 1963 [9], the unpredictable behavior of the atmospheric convection simulation model was the first example of a non-linear dynamical system, which is strongly dependent on the initial

state and characterized by a strange attractor in phase space. There were lots of other dynamical systems described after, which are governed by non-linear differential equations and correspond to different physical phenomena (e.g., Rössler system [10, 11], Chen system [12], etc). An example of a discrete chaotic oscillator, based on a matrix structure is analyzed in the work [13]. Numerically chaos can be assessed by Lyapunov exponents, which provide characteristics of chaotic signal pulsations as an exponential difference between two initially close trajectories [14]. In 1999, developing a linear partial state-feedback controller, which allows deriving the Lorenz system from a non-chaotic state to be chaotic, Chen found a new chaotic system [15, 16]. The system is competitive with the Lorenz system in the structure, is topologically not equivalent to it, and has more complex dynamical behavior [17].

Using nonlinear dynamics methods in signal analysis and processing is reasonable even for signals without a precise model of their source. E.g., in biomedicine, in some cases, it is useful to assume that the processing signal has been generated by an unknown dynamic system to reconstruct a phase space and get a set of equations to build a computer model [18]. The problem of processing such signals is complicated by the influence of several regulatory mechanisms on the circulatory system, which leads to the heart rhythm variability, so even in a restful state, the characteristics of fluctuations correspond to the state of dynamic chaos. In common cases, pulse wave signals could be random and unstable, which corresponds to the chaotic behavior of a dynamic system.

Not only could natural phenomena demonstrate chaotic behavior, but even simple electrical oscillation circuits can be applied to obtain complex output signals. Thus, for instance, Ku and Sun described the chaotic behavior of Van der Pol oscillator [19]. In 1983 Chua proposed an electrical circuit that became an example of a classical chaotic oscillator. The scheme consists of a linear oscillating LC-circuit with a non-linear negative resistance called a Chua diode [20, 21]. It was also shown that transistor-based circuits, like Colpitts or Hartley oscillators, can produce chaotic signals [22-24]. There are lots of other chaotic oscillator implementations described in the literature (e.g., in works [25-29]): from simple microcontroller-based oscillators and random bit generators (e.g., presented in papers [25, 26]) to complex FPGA-based chaotic cryptosystems [27]. An analog Lorenz

circuit and its radio frequency implementation are presented by Blakely, Eskridge, and Corron. They propose a simple schematic design, which can produce chaotic oscillations with a peak frequency equal to 930 kHz and significant power beyond 1 MHz [28]. Some approach to simplifying chaotic circuits with quadratic nonlinearity was proposed in the work [29], whereby a chaotic system with quadratic terms is realized using only a few multipliers and passive linear elements.

Discovered in 1990 by Pecora and Carrol, the capability of chaos synchronization [30] facilitated chaos-based telecommunication application development. In spite of the high dependence on initial conditions, which means that two initially close phase trajectories with time become uncorrelated, it is possible to synchronize two dynamical systems in order to make them evolve identically. For instance, the regime of unidirectional synchronization of two coupled dynamical systems (primary and secondary) could be set up following the method, proposed by Pecora and Carrol, whereby each original system must be decomposed into two subsystems. The primary system keeps its autonomy and self-oscillating abilities, while the secondary system becomes non-autonomous and driven by the synchronization signal that comes from the primary system [30, 31]. Influenced by a control signal, secondary system phase trajectories with time tend to primary ones making a "chaotic response". Of course, there are lots of limitation factors, which destabilize and prevent synchronization. For instance, parameters of primary and secondary systems must be equal as far as it is possible to set up a complete synchronization regime. Another example of such destabilization is noise influences in the channel [32]. Studying synchronization of Lorenz systems, Liao and Lin showed that not all state variables can be used as a driving signal [33]. Thus, using the first and second variables would allow coupled Lorenz systems to get synchronized, but not the third one [33, 34]. The synchronization phenomenon is a crucial aspect in various chaotic applications, which include novel data transceiving approaches, information security, measuring devices, signal detection application, model data parameter estimation, and prediction [35]. In telecommunication systems chaotic signals are used as carriers for information signals. One of the simplest ways of sending an analog signal is called "chaotic masking", whereby the sender adds a message to a chaotic signal and sends

this sum via a communication channel. Following this approach, the amplitude of the chaotic carrier must be much higher than the amplitude of the information signal. Examples of masking are exhibited in works [36-37]. In the work [36] authors proposed a combined scheme of chaotic modulation, recursive encryption, and chaotic masking. A model of high secure multichannel radio communication system based on the Rucklidge dynamical system was exhibited in the work [37]. Another approach involves changing one of the primary system parameters to transmit a binary signal by switching the secondary system from a synchronized regime to a desynchronized one and vice versa [35]. Thus, data transmitting using chaos requires mixing an information signal with a chaotic carrier. This procedure performs data encryption and spreads the spectrum of an information signal, which increases information security and allows sending the same amount of data with a much smaller power used [38].

Security algorithms [39], which are based on dynamical chaos theory, have shown good properties in many relative aspects of telecommunications and data transmitting technologies due to their superiority over ordinary random number generators [40, 41].

As a result of the brief overview, we should admit the potential of a broad area of practical use of dynamical chaos applications, especially in any kind of info-communication system and Internet Of Things (IoT) design, however, in this present work we confine our research to the use of a known dynamical system (Chen system) to perform analog signal transmissions.

3.2. Mathematical model of chaotic transceiver

Let us consider a continuous dynamical system that evolves governed by the following vector equation:

$$\frac{d\bar{u}(\tau)}{d\tau} = \bar{F}\left[\bar{u}(\tau), \bar{k}\right], \quad \bar{u}(\tau) \in R^n, \quad \bar{k} \in R^m, \tag{3.1}$$

where $\bar{u}(\tau) = \left[u_1(\tau), u_2(\tau), \cdots, u_n(\tau)\right]$ is a state vector of the system, $\bar{k} = \left[k_1, k_2, \cdots, k_m\right]$ is a vector of parameters, and $\bar{F}$ is a non-linear vector function

which is assumed to be known on both transmitting and receiving sides.

According to the decomposition method [30], the original system (3.1) is supposed to be separable into two subsystems:

$$\bar{F} = \left[\bar{G}, \bar{H}\right], \quad \bar{u} = \left[\bar{v}(\tau), \bar{w}(\tau)\right], \tag{3.2}$$

where

$$\bar{v}(\tau) = \left[u_1(\tau), u_2(\tau), \cdots, u_p(\tau)\right], \ \bar{w}(\tau) = \left[u_{p+1}(\tau), u_{p+2}(\tau), \cdots, u_n(\tau)\right],$$

$$\bar{G} = \left[F(\bar{u}), F(\bar{u}), \cdots, F(\bar{u})\right],$$

$$\bar{H} = \left[F_{p+1}(\bar{u}, \bar{k}), F_{p+2}(\bar{u}, \bar{k}), \cdots, F_n(\bar{u}, \bar{k})\right].$$

Thus, equation (1) can be rewritten as follows:

$$\begin{cases} \dfrac{d\bar{v}(\tau)}{d\tau} = \bar{G}\left[\bar{v}(\tau), \bar{w}(\tau), \bar{k}\right] \\ \dfrac{d\bar{w}(\tau)}{d\tau} = \bar{H}\left[\bar{w}(\tau), \bar{w}(\tau), \bar{k}\right] \end{cases}, \quad \begin{matrix} \left[\bar{v}(\tau), \bar{w}(\tau)\right] \in R^n \\ \bar{k} \in R^m \end{matrix} \tag{3.3}$$

where $\bar{v}(\tau)$ and $\bar{w}(\tau)$ are state vectors of first and second subsystems, respectively.

Now let us get two identical dynamical systems decomposed with the rule (2). The first system is a primary (P) or a driver system, whereas the second one is a secondary (S) or a response system. The primary and the secondary systems are assumed to be constructed on the transmitting and the receiving sides, respectively.

Hence, the complete synchronization of two coupled non-linear systems is described as follows:

$$\begin{cases} \dfrac{d\bar{v}_{PD}(\tau)}{d\tau} = \bar{G}\left[\bar{v}_{PD}(\tau), \bar{w}_P(\tau), \bar{k}_P\right] \\ \dfrac{d\bar{w}_P(\tau)}{d\tau} = \bar{H}\left[\bar{v}_{PD}(\tau), \bar{w}_P(\tau), \bar{k}_P\right] \\ \dfrac{d\bar{v}_S(\tau)}{d\tau} = \bar{G}\left[\bar{v}_{PD}(\tau), \bar{w}_S(\tau), \bar{k}_S\right] \\ \dfrac{d\bar{w}_S(\tau)}{d\tau} = \bar{H}\left[\bar{v}_{PD}(\tau), \bar{w}_S(\tau), \bar{k}_S\right] \end{cases}, \tag{3.4}$$

$$\left[\bar{w}_{P,S}(\tau), \bar{v}_{PD,S}(\tau)\right] \in R^n, \quad \bar{k}_{P,S} \in R^m$$

Here vector $\overline{v}_{PD}(\tau)$ from the primary system is set to be a driving signal (D). However, not all possible variances of the state vector can be used as a driving signal [28, 29].

Let us define the synchronization error $\varepsilon(\tau)$ as a difference between the signal $\overline{w}_P(\tau)$ coming from the primary system, and the output signal $\overline{w}_S(\tau)$ generated by the secondary system:

$$\varepsilon(\tau) = \left\| \overline{w}_P(\tau) - \overline{w}_S(\tau) \right\|. \tag{3.5}$$

Thus, setting up the synchronization regime means asymptotical decay of the error:

$$\lim_{\tau \to \infty} \left\{ \varepsilon(\tau) \right\} \to 0. \tag{3.6}$$

The last statement can be achieved if all the Lyapunov exponents of the secondary system are negative under driving signal control [30, 31].

The Chen [12] system consists of three non-linear differential equations:

$$\begin{cases} \dfrac{dx_1}{d\tau} = a(x_2 - x_1) \\ \dfrac{dx_2}{d\tau} = (c-a)x_1 - x_1 x_3 + c x_2, \\ \dfrac{dx_3}{d\tau} = x_1 x_2 - b x_3 \end{cases} \tag{3.7}$$

where *a*, *b*, and *c* are real system parameters [8, 11-13].

Let us denote a vector function of the right parts of the system (3.7) as $\overline{Y}(x_1, x_2, x_3)$. Thus, the system is dissipative if $div\overline{Y}(x_1, x_2, x_3) < 0$. For the Chen system, the dissipation condition is inequation:

$$c < a + b \tag{3.8}$$

Equilibrium points of the Chen system are estimated by setting $\overline{Y}(x_1, x_2, x_3) = 0$. Hence, the system has three equilibrium points: $P_0(0,0,0)$ (trivial), and $P_{1,2} = \left(\pm\sqrt{b(2c-a)}, \pm\sqrt{b(2c-a)}, 2c-a \right)$. For the Chen system, nontrivial equilibrium points exist if $c < a/2$.

The stability of a dynamical system is determined by the signs of the Lyapunov exponents at each point of the phase trajectory, depending on initial conditions and its current state (for $t = t_0$). Hence, the Lyapunov exponents in terms of a distance between two initially close trajectories are defined by the expression:

$$\bar{\lambda} = \lim_{t\to\infty}\left\{\frac{1}{t-t_0}\log\left[\frac{m(t)}{m(t_0)}\right]\right\}, \tag{3.9}$$

where $\bar{\lambda}$ is the a vector of Lyapunov exponents and m is the distance between phase trajectories.

According to expression (3.9), the distance changes exponentially with time, and non-negative Lyapunov exponents show system stability. Once the highest Lyapunov exponent reaches a positive value, it means the chaotic behavior of the system [14].

For the system (3.7), let us define a control parameter as

$$p = a - c, \tag{3.10}$$

then, setting parameters a and b equal 3 and 50 respectively, a chaotic regime is set up for the range $p \approx (7.5;\ \ 15.0)$ (see Fig. 3.1). Hence, for this range of the control parameter, fragments of bifurcation diagrams for each state variable are filled due to period doubling (Fig. 3.1, a), and the highest Lyapunov exponent λ_1 is positive (Fig.3.1, b).

Having been solved numerically by the Runge-Kutta method, phase portrait examples of the Chen system for different values of the control parameter are shown in Fig. 2, where points $I_{1,2}$ are two sets of initial conditions and $P_{1,2}$ are equilibrium points for each example. The set of equations (3.7) provides the Chen system of dimensionless values of state variables. To expand this abstract mathematical model to a dynamic system, described in physical terms, the next set of coefficients has been introduced:

$$\begin{aligned} x_i &= \mu_i V_i, \quad dx_i = \mu_i dV_i \\ \tau &= \mu_T t, \quad d\tau = \mu_T dt \end{aligned} \quad (i = 1\ldots 3) \tag{3.11}$$

For instance, to have state variables in volts and time in seconds, dimension units of coefficients μ_i and μ_T must be $[V^{-1}]$ and $[s^{-1}]$ respectively. Thus, a, b, and p are

proportional coefficients keeping their dimensionless values:

$$k_1 = a\frac{\mu_T\mu_2}{\mu_1}, \quad k_3 = p\frac{\mu_T\mu_1}{\mu_2},$$
$$k_4 = \frac{\mu_T\mu_1\mu_3}{\mu_2}, \quad k_6 = \frac{\mu_T\mu_1\mu_2}{\mu_3}, \qquad (3.12)$$
$$k_2 = a\mu_T, \quad k_5 = c\mu_T, \quad k_7 = b\mu_T$$

where k_i – are coefficients of a physical model.

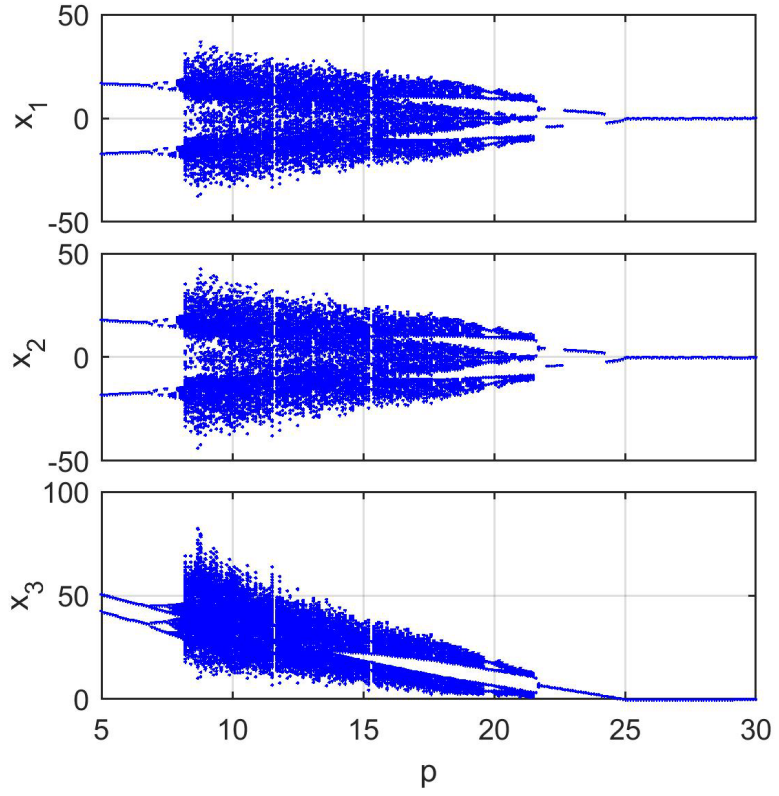

(a)

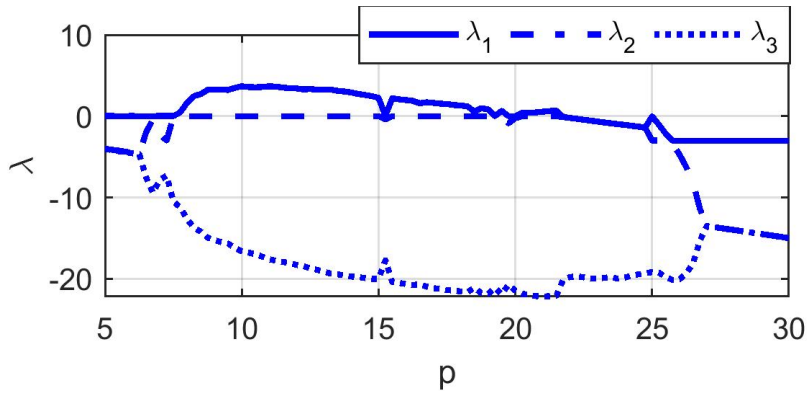

(b)

Figure 3.1 – Bifurcation diagrams (a) and Lyapunov exponents (b) of the Chen system for the range of control parameter (a = 50, b = 3, $c = a - p$)

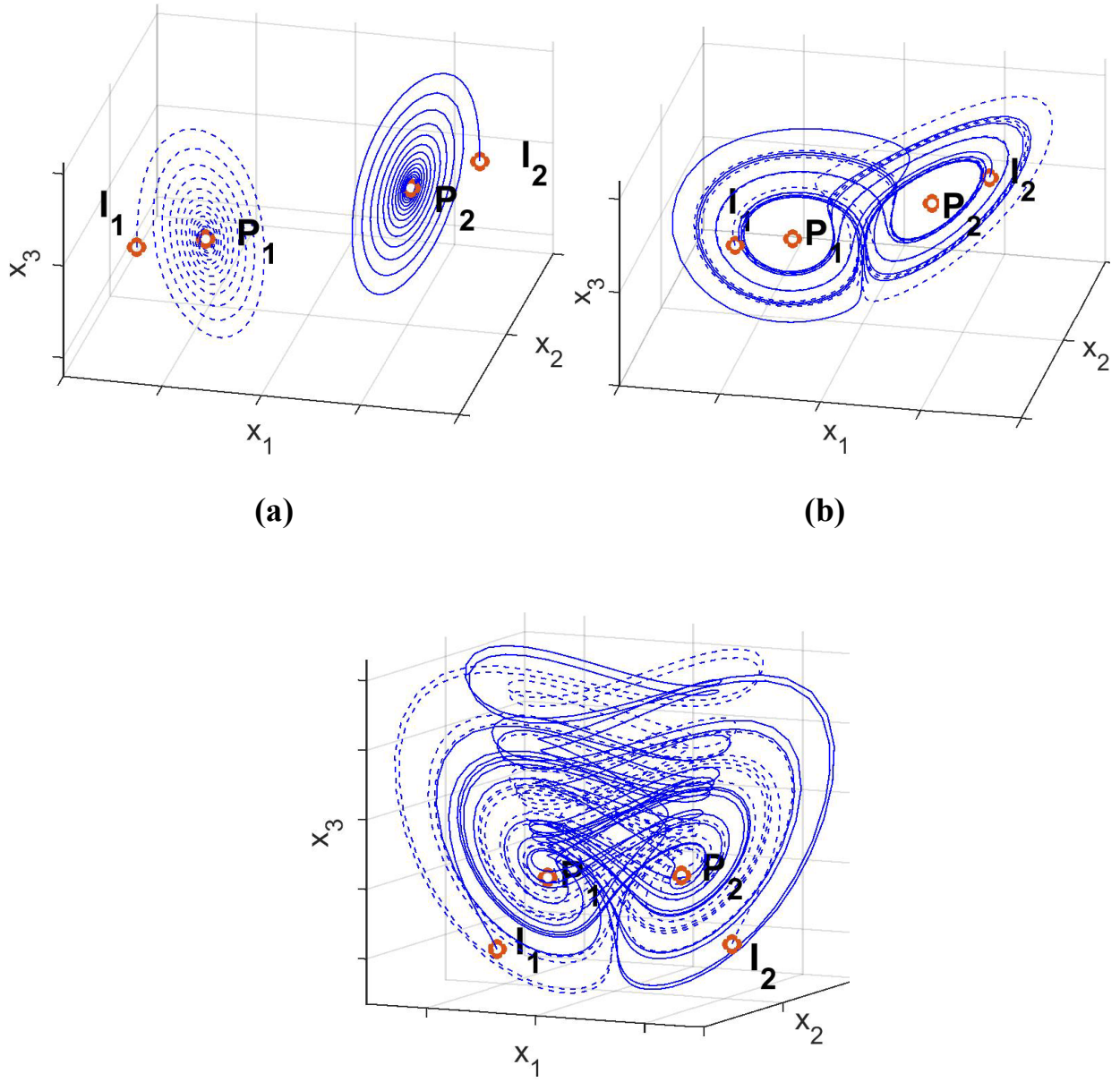

Figure 3.2 – Phaseportrait examples of the Chen system for different value of control parameter (assuming a = 50 and b = 3):
fixed points (a), p = 22.1, $I_{1,2}$ = (±7.000; ±7.000; 6.000),
$P_{1,2}$ = (±4.171; ±4.171; 5.800),
limit cycles (b), p = 19.5, $I_{1,2}$ = (±10.373; ±10.878; 12.055),
$P_{1,2}$ = (±5.745; ±5.745; 11.000),
chaotic attractor (c), p = 10, $I_{1,2}$ = (±16.439; ±17.621; 19.894),
$P_{1,2}$ = (±9.487; ±9.487; 30.000)

Applying substitutions (3.11) and (3.12) to the system (3.7) with (3.10), we get the Chen system represented in terms of an electrical circuit:

$$\begin{cases} \dfrac{dV_1}{dt} = k_1 V_2 - k_2 V_1 \\ \dfrac{dV_2}{dt} = -k_3 V_1 - k_4 V_1 V_3 + k_5 V_2 \\ \dfrac{dV_3}{dt} = k_6 V_1 V_2 - k_7 V_3 \end{cases} \quad (3.13)$$

where $k_{1\ldots7}$ are coefficients of the physical model.

Applying an analog integrator for the circuit implementation of i-th equation of set (3.13), we have got the expression for the output voltage:

$$V_i = -\int \left[\sum_{n=1}^{N} \frac{V_n}{k_{n,i}} \right] + V_i(0), \quad (i = 1 \cdots 3) \quad (3.14)$$

where N is a number of k-V-terms which occur is the right side of the given equation of the system (3.13), $V_i(0)$ is the initial charge of the capacitor, and coefficients $k_{n,i}$ are expressed in terms of equivalent resistances and capacitances: $k_{n,i} = 1/(R_n C_i)$.

The relevant inverting integrator, which is based on operational amplifier and represents the i-th equation of set (3.13), is shown in Fig. 3.3.

3.3. Difference-frequency signal transmitting and circuit implementation of Chen system

The chaos synchronization model has been applied to transmit a frequency modulated signal obtained from a difference-frequency block of pressure quartz sensor transducer. This application is an extension of the use of piezoresonance mechanotrons (PRMTs), which contains an interelectrode gap modulated by mechanical force [3, 4, 7]. The proposed design is represented by the block diagram which is shown in Fig. 4. The transmitting side (see Fig.3.4, a) consists of three main parts: a sensor circuit (SC)

connected with a quartz sensor, a difference frequency shaping circuit (DFSC), and a chaotic transmitting circuit (CTC). In the sensor circuit, the sensor is connected directly to the PRMT-based pressure measuring transducer, which is connected to the oscillator (OC) and included in the oscillation system.

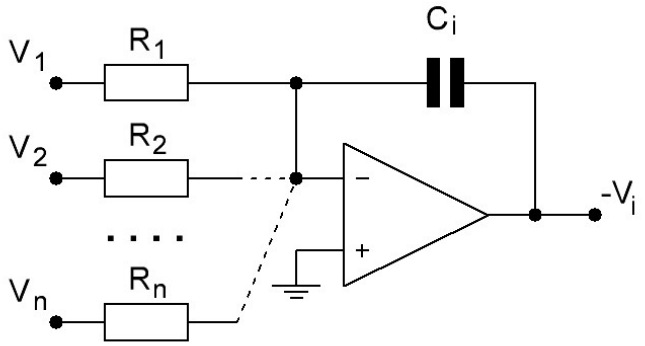

Figure 3.3 Equivalent branch current integrator based on operational amplifier

The aim of the DFSC is frequency converting and measuring process control during the measuring. Thus, input pressure changes ΔP(t) lead to the deviation of sensor circuit output frequency:

$$f = f_0 \pm \Delta f_{\text{inf}} \tag{3.15}$$

where f_0 is the rated frequency; Δf_{inf} is the frequency deviation, which provides information about the measured signal.

The raw output signal f is characterized as a low-deviation frequency-modulated signal. As a consequence, the process of demodulation could be complicated [1, 3]. In order to tackle this issue by increasing informational signal deviation, a frequency multiplier (FM) has been used. Multiplied frequency f_{m}, which is FM-block output signal, is mixed by mixer-block (MX) with reference frequency f_{ref}, generated by a direct digital synthesizer (DDS). Hence, the difference frequency is represented by the following expression:

$$f_{diff} = f_{ref} - f_m = f_{diff_0} \pm \Delta f_{diff} \tag{3.16}$$

where f_{ref} is the DDS output frequency; $f_{diff_0} = f_{ref} - n \cdot f_0$ is the difference frequency rated value; $\Delta f_{diff} = \pm n \cdot \Delta f_{\text{inf}}$ is the difference frequency informational component; n is a frequency multiplying coefficient.

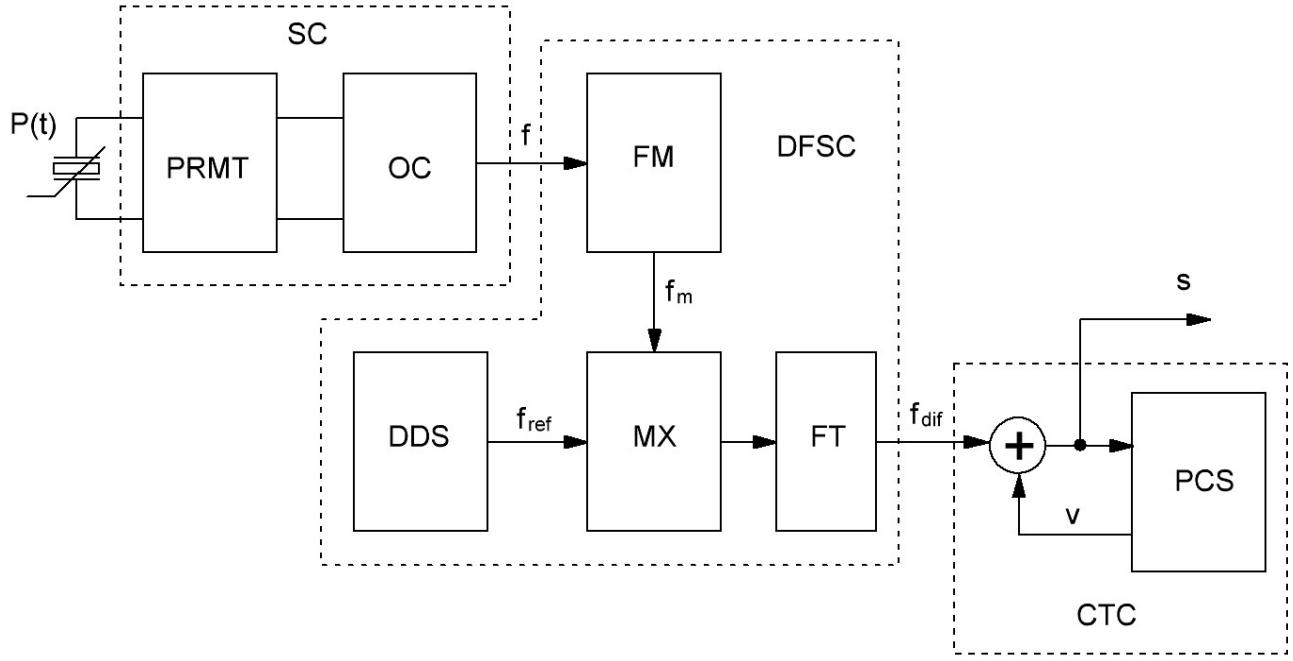

(a)

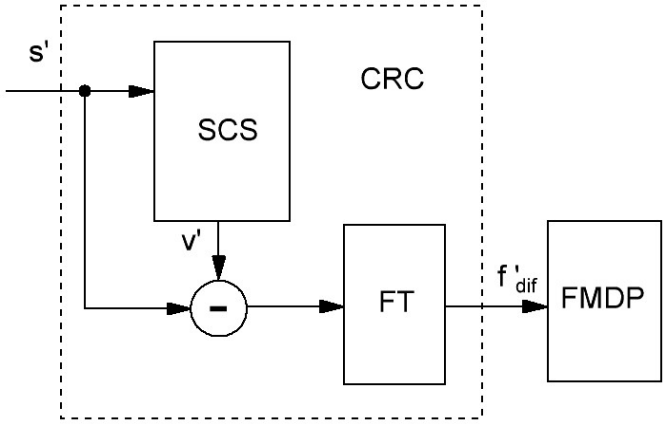

(b)

SC – Sensor Circuit
PRMT – Piezoresonance Mechanotron
OC – Oscillating Circuit
DFSC – Difference Frequency Shaping Circuit
FM – Frequency Mixer
DDS – Direct Digital Synthesizer
MX – Mixer
FT – Filter
CTC – Chaotic Transmitting Circuit
PCS – Primary Chaotic System
CRC – Chaotic Receiving Circuit
SCS – Secondary Chaotic System
FMDP – Frequency Measuring Data Processor

Figure 4 – Block-diagram of chaotic transceiver for difference frequency transducer: transmitting (a) and receiving (b) sides

Having passed through filter circuits (FT), filtered and shape-formed difference frequency signal f_{diff} comes to CTC based on primary chaotic system (PCS). For this example, the second state variable (V_2) of the Chen system (3.13) has been used to mix

it with the informational signal:

$$s = v + A\sin\Psi \tag{3.17}$$

where A and Ψ are amplitude and phase of informational signal, respectively, $v = V_2$ – is a modulated state variable.

Thus, signal s is transmitted via a communication channel and comes to the receiving side as signal s' (see Fig. 3.4, b).

On the receiving side, a chaotic receiving circuit (CRC) consists of a secondary chaotic system (SCS) and FT modules. The signal f'_{diff} is demodulated by subtracting from income signal s' the state variable v', generated by SCS as it is shown in Fig. 3.4, b.

Finally, the demodulated signal of the difference frequency f'_{diff} comes to the frequency measuring data processor (FMDP) in order to estimate its period and convert it into digital code according to the procedure T_{diff} (ΔP) → N_{code}(ΔP) for post processing.

The circuit model of two connected Chen oscillators has been built using Multisim software, which uses the PSpice model to simulate electrical components (Fig. 3.5). Ideal operational amplifiers and analog multipliers have been picked from the Multisim component library. The circuit consists of three analog integrators, built of operational amplifiers $U1$-$U3$ for each dynamical systems (primary and secondary) according to eq. (3.13) and Fig. 3.3, with a set of passive R-C-components for each integrator. Values of passive components are also shown in Fig. 3.5. Operational amplifiers $U4$, $U8$, and $U9$ are used as an inverting block to get the control signal V_2 inverted.

Obtained after simulation, strange attractors of the primary and secondary systems are displayed in Fig.3.6, a, b respectively.

Under the regime of complete synchronization, the phase portrait in the plain plane $V_{\text{p},2} - V_{\text{s},2}$ of driving signal $V_{\text{p},2}$ and signal $V_{\text{s},2}$ produced by the secondary system has a form of a straight line with a slope of 45° (with equal scales of each axis). Any distortions of the phase portrait are caused by system parameters inequality, noise influence, or (in the case of a computer simulation) simulation errors (Fig. 3.6, c).

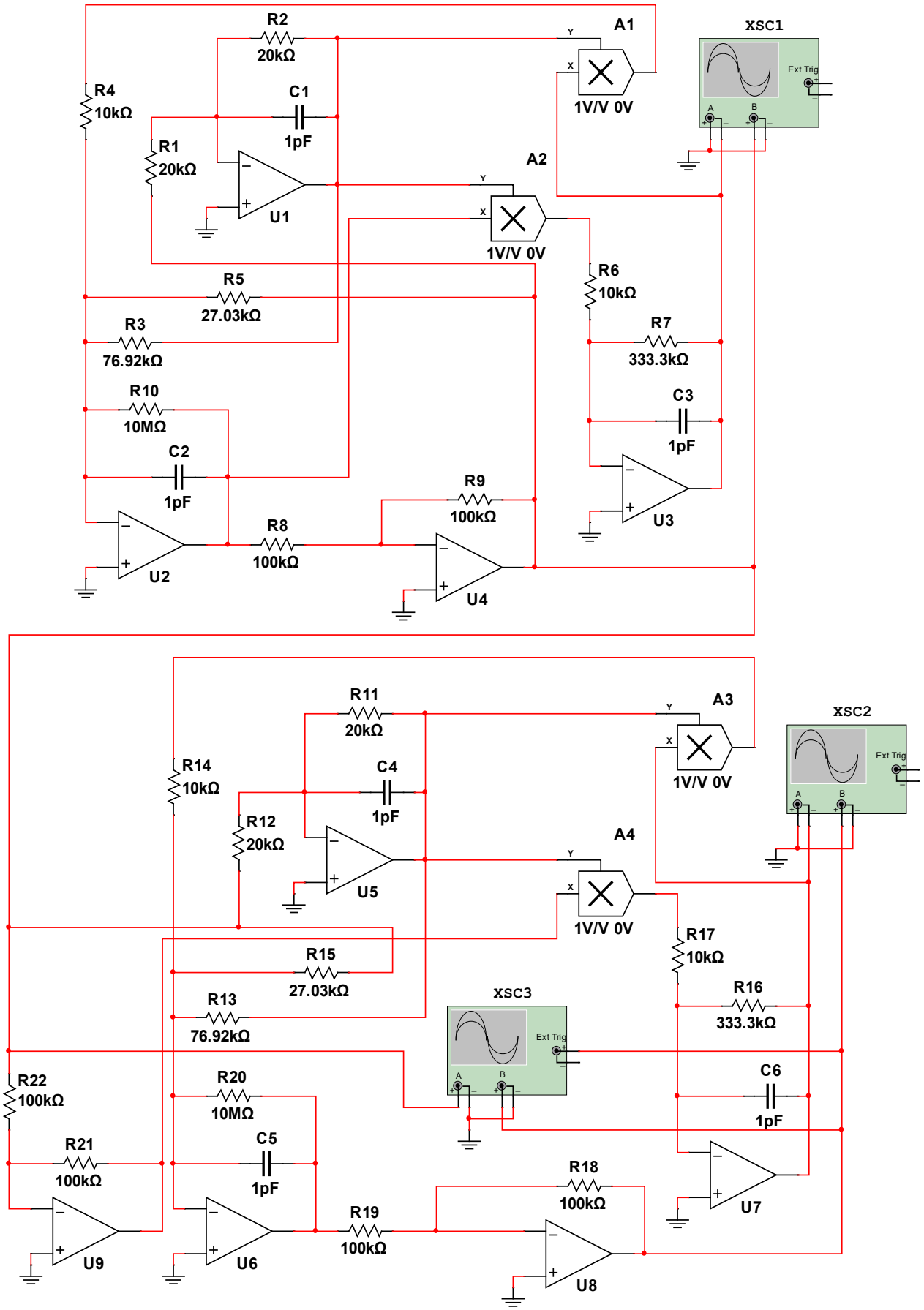

Figure 3.5 – Simulation circuit model of two connected Chen oscillators built using Multisim software

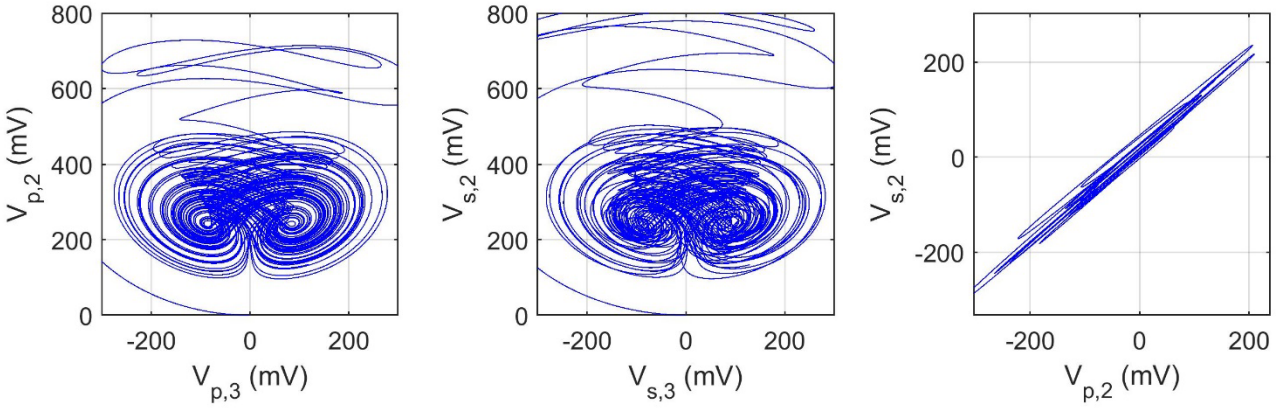

(a) **(b)** **(c)**

Fig. 6. Circuit simulation results: strange attractors of the primary (a) and the secondary (b) systems built in phase plane $V_3 - V_2$; phase portrait in plane $V_{p,2} - V_{s,2}$ of driving signal $V_{p,2}$ and signal $V_{s,2}$ produced by the secondary system (c)

Conclusions

As a conclusion of the chapter, the following statements have been formulated:

1. The prospect of using devices with chaotic dynamics in modern telecommunication and telemetry applications is due to a number of factors, including high information capacity, a wide range of frequencies, and confidentiality of messages. The possibility of implementing on the basis of one device a large number of chaotic modes in the future makes it possible to build multi-channel information transmission systems. High dependence on initial conditions and instability of phase trajectories allows to control the dynamics of chaotic generators and to carry out modulation with high speed due to small influences.

2. Despite the simplicity of implementation, the method of transmitting, whereby an informational signal is mixed with a chaotic carrier, design, and practical realization of such devices requires managing many issues. Two of them are component inequality and noise influence, which lead to non-linear distortion of transmitted signal preventing setting the synchronization regime.

3. The described approach can be applied to the multichannel transmission of narrowband signals with angular modulation, for example, in wireless info-communication and telemetry systems using quartz sensors, which are based on signal transducers with frequency output.